Imaging Device that Uses the Wavelet Transformation as the Image Reconstruction Algorithm. II. The *L* Transform

John H. Letcher

Department of Computer and Mathematical Sciences, University of Tulsa, 600 South College, Tulsa, Oklahoma

ABSTRACT

An ultrasound-device image-reconstruction algorithm has been described previously that uses orthonormal wavelets as the basis of a transform space. The transform algorithms make it possible to analyze the reflected ultrasound signal from a sample to produce a map of one of its internal properties, the acoustical impedance. Conventional wavelets do not exhibit translation invariance, the lack of which ofttimes generates nonzero expansion coefficients for wavelets of lower sequency than the transmitted signal. By a transformation of basis to a set of functions which exhibit a form of translation invariance the aforementioned problem is removed. However, the new functions are no longer orthogonal. An algorithm is described to perform this transformation extremely efficiently. Also described is an algorithm to unsmear the image due to the fact that the transmitted signal may not be a single wavelet but instead is a short sequence (linear combination) of wavelets. The coefficients of the array used to deconvolve the signal are determined by performing a forward wavelet transformation on the transmitted signal itself. © 1994 John Wiley & Sons, Inc.

I. INTRODUCTION

In the previous article in this series [1] it was shown that by sending a finely focused beam of sound into a body which consists of a single wavelet, it is possible to use the wavelet transformation to reconstruct maps of the acoustical impedances within the body from the received time series which are digitized values of the reflected sound. Signal conditioning was performed in the previous article to prevent the wavelet transformation from calculating nonzero expansion coefficients for wavelets of lower sequency than any that are present in the transmitted signal. This article presents a technique to correct the results of the wavelet transformation on data on which conditioning has not been performed. As will be shown, this doubles the resolution of the imaging device.

Placing stern constraints upon the shape of the transmitted wavelet (which was done in the first article) may not be practical due to variations in parameters of commercially available transducers, or the complexity of the circuitry required to implement the precise pulse shaping. It should be possible to measure the response of any transducer and employ techniques akin to inverse filtering to correct the received signal to become that which would have been received had the transmitted signal been a single wavelet. This article presents one such technique. The next article in this series will deal with a number of such techniques (deconvolution) in detail.

II. ORTHONORMAL WAVELETS

Given a positive integer M, consider a set of numbers $\{C_k\}$ where C_k is nonzero for $k = 0, \ldots, M-1$ and $C_k = 0$ otherwise. We may also consider the scaling function defined by the dilation equation

$$\phi(x) \equiv \sum_{k=0}^{M-1} C_k \phi(2x - k) . \tag{1}$$

Using this scaling function, a wavelet may be defined thus:

$$W(x) \equiv \sum_{n=0}^{M-1} (-1)^n C_n \phi(2x - 1 + n) . \tag{2}$$

If the values of the set of coefficients $\{C_k\}$ are correctly chosen, then it can be achieved that

$$\int \phi(x)\, dx = 1 , \tag{3}$$

$$\int W(x)\, dx = 0 , \tag{4}$$

$$\int |W(x)|^2\, dx = 1 , \tag{5}$$

$$\int \phi(x) W(2^j x - k)\, dx = 0 , \quad j, k \in Z , \tag{6}$$

and

$$\int W(x) W(2^j x - k)\, dx = \delta_{j0}\delta_{k0} , \quad k \in Z . \tag{7}$$

The values of the sets of coefficients are far from arbitrary. It is found that M is an even number, and for $M = 2$, the only solution is where $C_0 = 1$, $C_1 = 1$, and $\phi(x) = 1$ when $0 < x < 1$, $\phi(x) = 0$ otherwise.

For $M = 4$, the only solution is where

$$C_0 = (1 + \sqrt{3})/4 , \quad C_1 = (3 + \sqrt{3})/4 ,$$

$$C_2 = (3 - \sqrt{3})/4 , \quad \text{and} \quad C_3 = (1 - \sqrt{3})/4 .$$

Received 19 February 1993; revised manuscript received 3 May 1993

International Journal of Imaging Systems and Technology, Vol. 5, 33–38 (1994)

CCC 0899–9457/94/010033–06

When $M = 2$, the Haar wavelet (called W_H) is produced and when $M = 4$, the D_4 (named in honor of Ingrid Daubechies) wavelet is generated. Other wavelets exist for $M = 6, 8$, etc.

III. *L* WAVELETS

For the purposes of this imaging device it is preferable to employ a set of basis functions, called L wavelets, which consist of the scaling function, the $N/2$ highest sequency wavelets, and $(N-2)/2$ other functions which are translates (with displacement $1/N$) of the first $N/2 - 1$ highest sequency wavelets. The new functions are placed halfway between the $N/2$ functions. This is shown in Fig. 1 for the Haar wavelet and the $M = 2$ L_2 wavelet. The subscript refers to the fact that for the wavelet shown, M has the value of 2.

If f represents a signal, then it can be represented by

$$f \approx \mathbf{W}_H^T \mathbf{B}_H \approx \mathbf{W}_L^T \mathbf{B}_L , \tag{8}$$

where $\mathbf{W}_H^T$ is a row vector consisting of the Haar wavelet functions and $\mathbf{W}_L^T$ is a row vector consisting of the L-wavelet functions. $\mathbf{W}_L^T$ is a row matrix which is the transpose of the column matrix $\mathbf{W}_L$. The array $\mathbf{B}_H$ is a column vector of expansion coefficients calculated by the wavelet transformation. The array $\mathbf{B}_L$ is the set of coefficients that the wavelet transformation would have produced had the basis functions been L wavelets.

Utilizing a space spanned by N basis functions (Haar wavelets), the basis functions are defined:

$$(W_H)_1 \equiv H_1 = \phi(1-x) \tag{9}$$

and for $n = 2, \ldots, N$ we define

$$(W_H)_n \equiv H_n = W_H(k - 2^j x) , \tag{10}$$

where $j = 0, \ldots, (\log_2 N - 1)$, $k = 1, \ldots, 2^j$ and $n = k + 2^j$. Therefore n takes on the values of all positive integers between 2 and N; i.e., $n = 2, \ldots, N$. The L wavelets for $M = 2$ are defined in a similar manner. That is,

$$(W_L)_1 \equiv L_1 = \phi(1-x) \tag{11}$$

and

$$(W_L)_n = W\left(\frac{n}{2} - 2^{\log_2 N - 1} x\right) , \tag{12}$$

where $n = 2, \ldots, N$.

The set of N functions $\{W_n\}$, $n = 1, \ldots, N$, made up of $\phi(1-x)$ plus $N-1$ functions $W(k - 2^j x)$ forms a basis for a space so that any reasonably well behaved function f can be accurately expressed as a linear combination of the basis

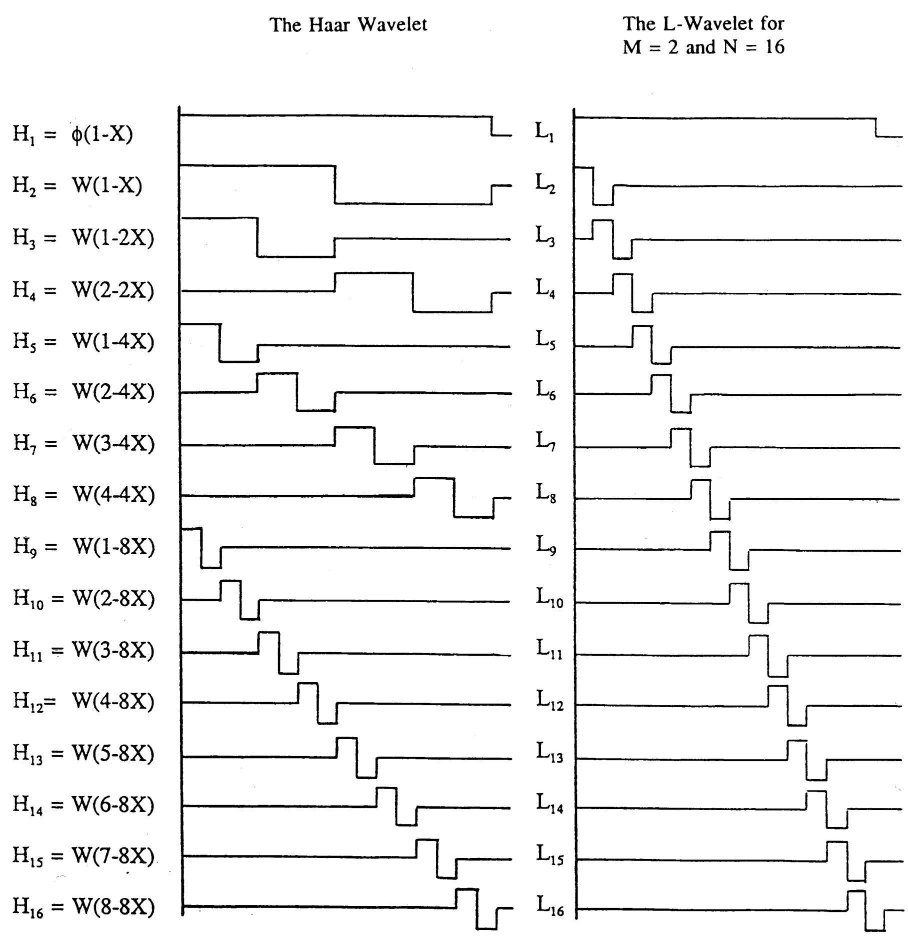

Figure 1. Plots of the amplitude of the Haar wavelet and the $M = 2$, $N = 16$, L wavelet as a function of time.

functions. That is,

$$f = \sum_{i=1}^{N} b_i W_i \, . \tag{13}$$

The function f is sampled at N evenly spaced points on the interval $[0, 1]$ thereby producing an array **F**. The wavelet transformation described in the previous article of this series [1] calculates the N-point array **B** from the N-point array **F** so that $(\mathbf{B})_n = b_n$.

Other L wavelets are possible for all even values of M and for all values of N as long as $\log_2 N$ is a positive integer. Notice that the L wavelets are not orthonormal. That is, the requirement of Eq. (7) is relaxed.

IV. *L* TRANSFORM

In the imaging device contemplated herein the $\mathbf{B}_H$ arrays are calculated from the received ultrasound signal. We now wish to transform bases so that the reflection coefficients refer to the L wavelets. By examining Fig. 1 it can be seen that this will double the resolution of the imaging process as $N-1$ reflection coefficients are calculated rather than $N/2$ as was calculated before.

If we premultiply Eq. (8) by $\mathbf{W}_H$ and integrate over all x, we have that

$$\mathbf{B}_H = \mathbf{W}_H \cdot \mathbf{W}_L^T \mathbf{B}_L \equiv \mathbf{D}\mathbf{B}_L \, . \tag{14}$$

Notice that $\mathbf{W}_H \cdot \mathbf{W}_H^T = \mathbf{1}$, the unit matrix, because the Haar wavelets are orthonormal. One can multiply Eq. (14) by $\mathbf{D}^T$ and define a matrix $\mathbf{S} \equiv \mathbf{D}^T\mathbf{D}$ so that

$$\mathbf{D}^T\mathbf{B}_H = \mathbf{D}^T\mathbf{D}\mathbf{B}_L = \mathbf{S}\mathbf{B}_L \, . \tag{15}$$

S is positive definite; therefore there exists an orthogonal (unitary) matrix **U** that diagonalizes **S**. That is,

$$\mathbf{U}\mathbf{S}\mathbf{U}^T = \mathbf{S}_D \, . \tag{16}$$

Since **U** is orthogonal, $\mathbf{U}\mathbf{U}^T = \mathbf{U}^T\mathbf{U} = \mathbf{1}$, so

$$\mathbf{D}^T\mathbf{B}_H = \mathbf{U}^T\mathbf{U}\mathbf{S}\mathbf{U}^T\mathbf{U}\mathbf{B}_L = \mathbf{U}^T\mathbf{S}_D\mathbf{U}\mathbf{B}_L \, . \tag{17}$$

Premultiplying both sides of Eq. (17) by **U**,

$$\mathbf{S}_D\mathbf{U}\mathbf{B}_L = \mathbf{U}\mathbf{D}^T\mathbf{B}_H \, . \tag{18}$$

So,

$$\mathbf{U}\mathbf{B}_L = \mathbf{S}_D^{-1}\mathbf{U}\mathbf{D}^T\mathbf{B}_H \, , \tag{19}$$

and finally we may define

$$\mathbf{B}_L = [\mathbf{U}^T \; \mathbf{S}_D^{-1} \; \mathbf{U} \; \mathbf{D}^T]\mathbf{B}_H \equiv \mathbf{L}\mathbf{B}_H \, . \tag{20}$$

In short, **L** is the inverse of **D**. The matrix **D** is determined from the properties of the $\mathbf{W}_H$ and $\mathbf{W}_L$ functions, alone. These do not vary; therefore **D** is calculated only once and **L** is calculated (only once) from **D**. Many zeros exist in the matrix **L**; therefore it is possible to generate computer code that carries out only the useful multiply and add operations of Eq. (20), thereby producing a sequence of instructions in which none of them is unnecessary. This is to say that Eq. (20) has been extremely efficiently coded. This process shall henceforth be called the L transform.

The orthogonal wavelet expansion coefficients, the values of which are held in the array $\mathbf{B}_H$, are calculated from the received sound signal **F** by the algorithms described in the previous article of this series [1]. Equation (20) is then used to calculate the L wavelet expansion coefficients, held in $\mathbf{B}_L$, from $\mathbf{B}_H$.

V. CALCULATION OF ACOUSTICAL IMPEDANCES FROM THE *L*-WAVELET EXPANSION COEFFICIENTS

In an ideal experiment, a perfect inverted Haar wavelet is produced by the transducer; that is, the amplitude of the sound produced over time is expressed by the equation for the Haar wavelet [given by one of the functions given in Eq. (11) or Eq. (12)] which is inverted by multiplying by -1. This inversion is equivalent to a time reverse of the wavelet and is necessary because as this signal is reflected from a boundary in the experimental sample, and second lobe (which is now positive) will be received first and properly interpreted as a (positive) Haar wavelet.

The width of the entire wavelet (both lobes of the wavelet) is defined to be $2T$. If an A scan desired is to produce 256 useful points in the image, then the useful period (the time over which useful data are received) is $256T$, expressed in seconds. The width of the scan D_{12} is expressed as the velocity of sound, v ($\sim 1.45 \times 10^5$ cm/sec multiplied by the useful period $256T$, which is $1.856 \times 10^7 T$ and divided by 2 (as a reflection must traverse a length *twice*). The sequency of the wavelet is $1/(2T)$. By waiting for an amount of time $\equiv hT$ before the scan begins, then the location of the left-hand side of the A scan is located at $D_1 = hTv/2$. The right-hand side of the A scan is located at $D_2 = (h + 256)Tv/2$. Again, $D_{12} = D_2 - D_1 = 128Tv$.

In practice, it is highly desirable to oversample the received signal; that is, if possible, at least ten data points are accumulated for each lobe of the Haar wavelet. This is difficult to achieve since for a 1-MHz Haar wavelet, the sampling rate of 20 MHz is required. Nevertheless, when the received time series is reduced to the array **P**, then the values of the received series are averaged over the time period of one lobe of the wavelet. If oversampling is performed by an amount N_p samples per array point, then the received signal (now held in an array **W**) is used to calculate the values of the received signal **P** by the following program fragment:

```
   DO 1 I = 1,N
   P(I) = 0.0
   ISTART = (I - 1)*NPTS
   DO 1 J = 1,NPTS
1  P(I) = P(I) + (W(ISTART + NSTART + J)/
          FLOAT(NPTS)
```

N has been given the value of 256, NPTS is the oversampling factor, N_p, and NSTART is the delay to select the portion of the signal to be analyzed.

If the transmitted signal is a pure Haar wavelet, $\mathbf{P} \equiv \mathbf{F}$; if not, a step is added to calculate **F** from **P** as given in the section on multiple wavelet transmission below.

In an ideal experiment using a sample (phantom) consisting of a single boundary between materials with acoustical impedance Z_1 and Z_2 then the received signal will be a wavelet with amplitude $Q(Z_2 - Z_1)/(Z_2 + Z_1)$. The constant of proportionality Q depends upon many things; however, it will be arbitrarily *adjusted* by varying the gain of the input amplifier so that the maximum signal received is with the bounds of the device analog-to-digital converter so that the range is not exceeded (which produces clipping) or is not enough (which hurts the signal-to-noise ratio). Once the value of Q is known, then the amplitude of the signal (which is the value of one of the **BL** array, the index of which corresponds to the depth of the boundary) is calculated and the array **V** of acoustical impedances may be calculated using the program fragment:

```
      BAVG = 0.0
      DO 5 I = 2,N
      BAVG = BAVG + BL(I)
    5 BAVG = BAVG/FLOAT(N - 1)

      V(1) = 1.0
      S = V(1)
      DO 6 I = 2,N
      BX = BL(I)
      BX = BX - BAVG
      S = S*(Q + BX)/(Q - BX)
    6 V(I) = S
```

Any good optimizing compiler will recognize that the variables Q, BAVG, S, and BX can be register variables, so this program fragment requires only N memory reads (from **BL**) and N memory writes (to **V**) after the values of Q and N have been loaded.

VI. USE OF SINGLE SINUSOIDS IN THE PLACE OF HAAR WAVELETS

The power spectrum of a signal is the Fourier transform of the autocorrelation function of the signal. For a single Haar wavelet (or any multiple thereof) the spectrum is unbounded. This makes a Haar wavelet *impossible* to generate exactly because no transducer is capable of generating extremely high frequencies. The Fourier transform of a regular square wave (the equivalent of a regular sequence of Haar wavelets) is also unbounded.

The question has been asked, what if the Haar wavelet is replaced by a single sinusoid, a sine wave of exactly one cycle, zero otherwise? A sequence of these (with no gaps) has a Fourier transform with expansion coefficients of only one frequency. A good sinusoid is what a typical ultrasound transducer is comfortable in producing. So, what would be the change in the procedures already introduced: notably, is the direct average of the oversampled signal still appropriate and accurate? To partially answer this question, a test data set was calculated and placed in the array **W** consisting of positive, then negative, sinusoids of amplitude 1.0 with 11 times oversampling [the sinusoid is defined $W(I + K) := \pm \sin(2\pi I/22)$ for $I = 0, \ldots, 22$]. The first sinusoid was placed at point 10 with sign +1, the next at point 10 + 111 with sign −1, and repeated throughout the interval of the 4096-point array with a spacing of 111. This array was subjected to the calculation

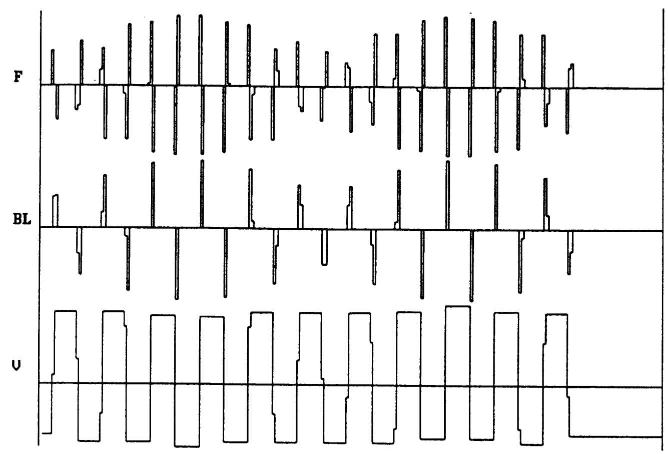

Figure 2. Plots of the calculated received signal, *L*-wavelet expansion coefficients, and the calculated acoustic impedance for the test signal described in the text.

processes described throughout and the results are displayed in Fig. 2. Notice that the plot of calculated acoustical impedances V is the square wave that we had expected, even though the sampling and average took place over all possible displacements of the sinusoids.

VII. MULTIPLE WAVELET TRANSMISSION

Oftentimes, it is impractical to use a pure (single) wavelet as the transmitted signal that is used by the imaging device. Instead, the signal produced by the transducer is a very short *sequence* of single wavelets of decreasing magnitude. That is, the transmitted signal is given by

$$\mathbf{T} = \sum_{n=1}^{m} d_n (\mathbf{W}_L)_{n+k}\,, \quad m \ll N\,, \tag{21}$$

where k is a number so that $(\mathbf{W}_L)_{1+k}$ is the first value that is nonzero.

The received signal from any sample ($\equiv$**P**) can be converted to a signal **F** which is that which would have been obtained had the transmitted signal been a single wavelet. This is equivalent to saying that

$$\mathbf{F} = \sum_{n=1}^{m} d'_n (\mathbf{W}_L)_{n+k} = (\mathbf{W}_L)_{1+k} \tag{22}$$

as $d_1 = 1$ and all others are zero.

The process of calculating **F** from **T** is given the generic name deconvolution. This is a complicated subject and will be addressed in detail in the next article in this series. For now it is only necessary to say that in a practical imaging device, a received signal **T** is obtained from a single sharp discontinuity in acoustic impedance in a phantom experimental subject consisting only of layers of water and layers of wax. In this experiment, the beam of sound is made to strike the layer perpendicular to the surface. The wavelet transformation is applied to the received signal and the **B** array of the transform gives the values of d_n directly. It can be seen that

$$d_n = (\mathbf{B})_{n+l}/(\mathbf{B})_{1+l}\,, \tag{23}$$

where $1 + k$ is the first element which is nonzero and $n =$

1, . . . , m and where $m \ll N$. An array **D** may be defined so that $(\mathbf{D})_n \equiv d_n, n = 1, \ldots, m$. By definition, $d_1 = 1.0$. In order to calculate the deconvolved signal to be contained in an array **F** from the received signal contained in an array **P** and using an array **D** calculated by the process, one may use the simple deconvolution algorithm shown by the FORTRAN program fragment:

```
      DO 2 I = 1,N
      F(I) = P(I)
      DO 2 J = 2,M
    2 P(I + J – 1) = P(I + J – 1) – (D(J)*F(I))
```

VIII. EXPERIMENTAL RESULTS

The equipment utilized in acquiring and analyzing the sound data reported herein consists of three parts. The first component is a commodity PC class computer equipped with a Cyrix 486DLC microprocessor and a Cyrix EMC 87 coprocessor, each run at 33 MHz. The image display is provided by an ATI VGA Wonder 512 graphics adapter attached to an NEC 5FG monitor. The second component is a Panametrics 500PR pulser-receiver connected by means of a single coaxial cable to a Panametrics 2.5-MHz V305SU F = 3" ultrasonic transducer. The same transducer is used for sending and receiving. The third component is comprised of circuits especially built which were to accept the received sound signal, amplify it, then sample it by means of a Sony CXA 1296P analog-to-digital converter. The digitized data are fed to a Fujitsu MB81C78A-35 static RAM. Additional circuitry is provided to interface the electronics to the ISA bus in the computer.

The data collection circuitry is controlled by a latched fedback memory finite-state engine [2, 3] which is operated at 40 MHz. Only two signals lead from the pulser-receiver to the interface electronics: (1) digital synchronization signal, which is used to report that a wavelet had been generated, and (2) the received analog sound signal. Upon receipt of the synchronization pulse, the interface circuitry samples the analog signal at the rate of 20 million samples per second for a duration of either 4096 points or 8192 points (1 point = 5×10^{-8} sec). This provides for ten times oversampling or 20 points for the duration of the wavelet. The input amplifiers in the interface circuitry are identical to that which is found on the Sony CXA 1296P PCB evaluation board, which is commercially available. The software for image capture, image reconstruction, and image display were written by the author. This was optimized to take advantage of the advanced features of the Cyrix EMC coprocessor. The time required to generate the wavelet and acquire the time series for analysis was always less than 2 ms. Image reconstruction is performed in approximately this amount of time.

Two phantoms were constructed by separating and holding three layers of jeweler's carving wax approximately 0.25-in. thick. These were placed approximately 1 in. apart. This assembly was placed in a beaker containing previously boiled water to which was added a drop of strong dishwashing detergent. The treatment of the water was necessary to prevent the formation of small gas bubbles on each interface layer and to make sure that the wax surface, although smooth, was properly wetted. Signals of received sound were recorded, stored, and analyzed. Wax and water were chosen because they approximate the acoustic impedances of fat and water in the human body, respectively.

To compare the results obtained by using the technique reported herein with older techniques, the phantom used in these studies was also imaged using an Acuson instrument, which is in use for medical purposes. The results of this study are shown in Fig. 3. The results of the new technique are shown in composite in Fig. 4. In the latter figure, a plot of the sampled sound signal, F, the L-wavelet expansion coefficients, BL, and the calculated acoustic impedance V are

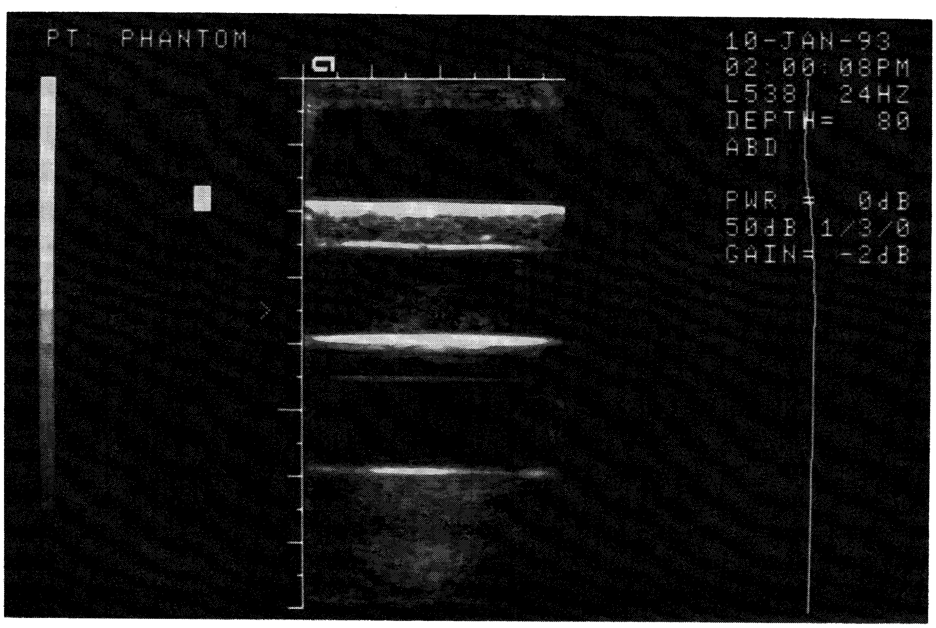

Figure 3. The image produced by an *A* cuson medical imaging device using the experimental wax/water phantom described in the text.

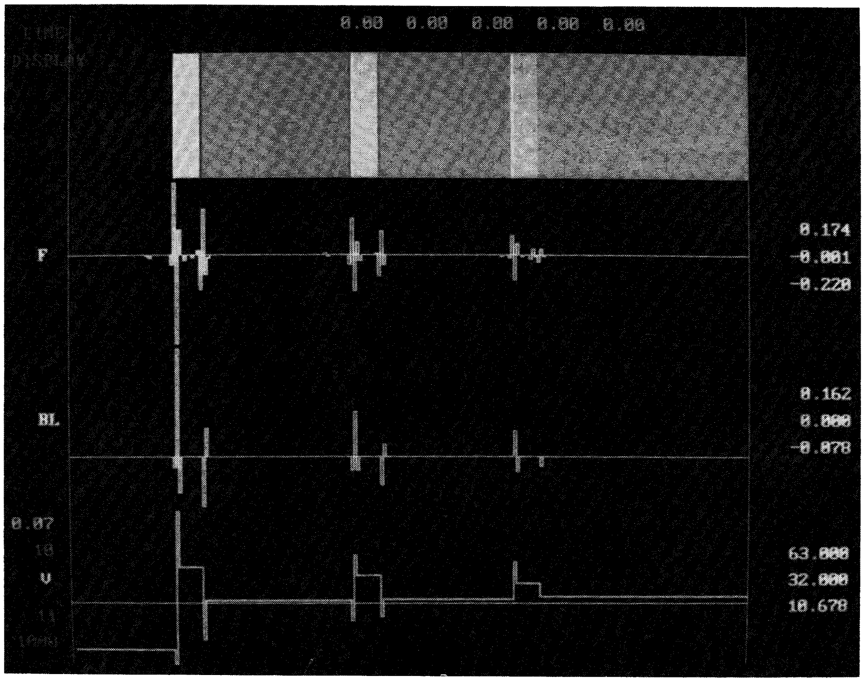

Figure 4. Plots of the 350 sample average of the received sound signal obtained using a wax/water phantom. Shown are the received signal, *F*, the *L*-wavelet expansion coefficients, and the calculated acoustical impedence *V*. Also shown is a density plot of the values of *V* shown on the same scale.

plotted against time. The image at the top of the figure is a density plot of V using scaling factors chosen by the author. No attempt was made to deconvolve the received signal due to an imperfection in the transmitted wavelet. This imperfection produced the overshoot in the calculated value of V at each boundary. This subject will be dealt with more fully in the next article in this series [4]. No attempt was made to account for absorption. Signal averaging of 350 samples produced this essentially noise-free image. Notice the sharp boundaries of the almost square wave for the acoustical impedances for the wax and water.

Noise is the limiting factor in the accuracy of this technique and great care should be exercised to keep the signal-to-noise ratio as large as possible. Oversampling at more than a factor of 10 seems unnecessary (except for further noise reduction).

REFERENCES

1. John H. Letcher, "An imaging device that uses the wavelet transformation as the image reconstruction algorithm. I," *Int. J. Imaging Syst. Technol.* **4**, 98–108 (1992).
2. John H. Letcher, "Clocked latched fedback memory finite state engines. I. A novel technique for the design of arithmetic and control processors," presented at Oklahoma Symposium on Artificial Intelligence, 3–4 November 1988 (unpublished).
3. John H. Letcher, "Clocked latched fedback memory state engine," United States Patent and Trademark Office, Patent No. 4786829, 22 November 1988.
4. John H. Letcher, Peyton Cook, and Kevin O'Neil, "An imaging device that uses the wavelet transformation as the image reconstruction algorithm. III. Digital filtering of imperfect wavelets, presented at the IEE London, 29 March–1 April 1993 (unpublished).